

Comb beam for particle-driven plasma-based accelerators

A. MOSTACCI(*)

*Dipartimento di Scienze di Base e Applicate per l'Ingegneria (SBAI)
Sapienza Università di Roma - Roma, Italy*

ricevuto il 6 Febbraio 2014; approvato l'1 Aprile 2014

Summary. — Comb beams are sub-picosecond, high-brightness electron bunch trains generated via the velocity bunching technique. Such bunch trains can be used to drive tunable and narrow band THz sources, FELs and plasma wake field accelerators. In this paper we present recent results at SPARC-LAB on the generation of comb beams for particle-driven plasma-based accelerators.

PACS 29.20.Ej – Linear accelerators.

PACS 29.27.Bd – Beam dynamics; collective effects and instabilities.

1. – Introduction

The SPARC photoinjector [1, 2] is based on a 1.6 cell *S*-band (2.856 MHz) rf gun which operates at high gradient, 120 MV/m peak on cathode. An UV laser pulse hits the copper cathode via an in-vacuum mirror placed at 50 cm from the cathode plane. The laser incidence angle on the cathode is about 2.5 degrees. The 300 μ J UV pulse is generated by a two stages CPA (Chirped Pulse Amplification) system seeded by a Ti:Sapphire oscillator [1]. The 50 mJ output infrared pulse is up-converted to 266.7 nm by using two non-linear crystals (BBO) and then sent to a transfer line for longitudinal and transverse flat top shaping. The emittance compensation process proceeds with the electron beam being focused by a solenoid just after the gun, and ends up at the exit of the subsequent 3 linac structures, where the energy is about 150 MeV. The entrance of the first accelerating section is placed at 1.5 meters from the cathode, where the local maximum of transverse emittance oscillations [3] coinciding with a beam waist ($\sigma' = 0$) was measured.

In order to prevent beam blow up during compression two long solenoids (TW solenoids) have been placed around the first two linac sections, as proposed in [4]. Each

(*) E-mail: Andrea.Mostacci@uniroma1.it

solenoid is composed by a long iron yoke containing 13 coils forming a long solenoidal magnetic field. The coils are grouped in triplets which can be separately powered (except for the first coil which has a stand alone power supply needed for fine field adjustments) [5]. With this flexibility the amplitude of the magnetic field on axis can be shaped longitudinally to optimize the beam envelope along the linac.

A diagnostic section after the 3 linac modules allows the measurement of beam properties: projected and slice beam parameters, both transverse and longitudinal, can be retrieved by the use of a rf deflector cavity (S band, 2.856 MHz), a spectrometer, and two quadrupole triplets [5]. The transfer line can be used to match the beam to the SPARC undulator for free electron laser amplification experiments. For time measurements the actual resolution is 90 fs at 150 MeV, limited by the maximum power feeding the deflecting cavity (1 MW). The energy resolution $\delta E_{min}/E$ is set by the dipole dispersion function and by the transfer line design, to 10^{-4} .

Due to the high versatility of the SPARC linac, important milestones has been set in the field of high brightness beam physics, such as emittance oscillations [3,6,7] and emittance compaction in RF compression [8], as well as in high brightness beam applications, such as FEL radiation from a chirped beam in the undulator [9].

Section 2 reviews the core technique used to create and manipulate high brightness beam at SPARC, *i.e.* the low-energy bunch compression (the so-called velocity bunching).

If a train of laser pulses illuminates the cathode (sect. 3), immediately after the cathode, there will be a train of electrons with the same energy if the injection phase is chosen properly. Because of space charge, the bunches lengthen and the original pulse structure is lost in the current profile. Nevertheless there is some memory of the original structure in the longitudinal phase space, as you can see in the energy modulation. By applying the velocity bunching and forcing a rotation in the phase space, one can recover at the end of the linac the original current modulation, that is generating a train of bunches with appropriate modulation.

This technique does not rely on any induced beam losses; therefore it has the potential advantage to go to high charge pulse train. The issue is the manipulation or the control of its properties, which can be done varying the machine parameters, as shown in sect. 4. Experimental results for a four pulses comb beam is reported in sect. 5 and some application are discussed in sect. 6.

2. – Velocity bunching at SPARC

The velocity bunching technique is a method for compressing an electron bunch by exploiting the interaction with the electromagnetic fields of an accelerating cavity. The theoretical model of the mechanism was described in ref. [4]. If a low energy beam (3–5 MeV) is injected in a traveling wave (TW) accelerating cavity close to the zero crossing phase (no acceleration), it accumulates rf-induced correlated velocity spread that tends to compress the beam (higher velocities to trailing particles); at the same time the bunch slips back to accelerating phases. Differently from the ballistic bunching, acceleration and compression take place simultaneously. The key point for beam compression is represented by the difference between the wave phase velocity and the beam mean velocity.

In principle it would be possible to find an equilibrium accelerating gradient which compensates the defocusing self-forces with the rf focusing and acceleration. Unfortunately such gradients are too high to be reached in present S -band TW cavities, so that further transverse focusing is needed to avoid beam expansion and transverse emittance blow up.

Systematic studies based on extensive beam dynamics numerical simulations have been carried out using the SPARC layout [1]. The key aspects of this compression technique such as the optimization of the magnetic field shape for the emittance compensation at different compression factors, the sensitivity to jitters and tolerances and the possibility to linearize the longitudinal phase space via an X-band cavity before the RF compressor to enhance the compression efficiency, have been studied. The importance of the velocity bunching in the context of the new photo-injector sources has already been exhaustively discussed elsewhere (see [8] and related reference)

3. – Comb beams

The required pulse shape of a comb laser beam is characterized by two or more short (hundreds of fs) pulses spaced by a few picoseconds. The technique used for this purpose relies on a birefringent crystal, where the input pulse is decomposed in two orthogonally polarized pulses with a time separation proportional to the crystal length. If more birefringent glasses are inserted in the laser beam path, it is possible to produce multi-peaks and a proper number of replicas to achieve a flat-top shape. For the measurement reported in this paper, the UV stretcher has been bypassed, and the short UV pulses have been sent to the birefringent crystal. The crystal is α -cut beta barium borate (BBO), which is a UV transparent optical material characterized by a strong birefringence. The α -BBO crystals are oriented with fast and slow axes at 45° with respect to the incident horizontal polarization, so that a single pulse is equally split into two pulses, with the orthogonal polarizations traveling at different group velocities in each crystal. Since the crystal has its optical axis parallel to the front surfaces, there is no spatial walk-off between the ordinary and extraordinary beams, and the output pulses are naturally aligned. The crystal thickness is 10.353 mm, thus inducing a separation between the pulses according to the following formula: $\Delta\tau = (n_e - n_o) L_1/c$. Here, L_1 is the BBO length, n_o and n_e are, respectively, the ordinary and extraordinary indexes of refraction at the wavelength of 266 nm, and c is the speed of light. For our crystal length, the pulse separation should be 8.15 ps. The birefringent material is coated with an antireflection superficial layer, and the energy losses can be limited to few percent. To adjust the pulse length, within the 0.5–2 ps range, a proper second-order spectral phase could be programmed by an acousto-optic programmable dispersive filter. Moreover, to change the relative intensity of the pulses, a remotely controlled half-wave plate is inserted before the BBO. This feature allows us to control the charge emitted by the two pulses and to compensate for the variation in the quantum efficiency associated with different gun extraction phases for the two pulses. After the birefringent crystal, a variable neutral filter is used to reduce the overall energy. For the present experiment, the total energy was 15 mJ. Interested reader can find additional details in ref. [10].

A comb laser pulse illuminating a photocathode in a RF gun can generate a train of short electron bunches. Downstream the photoinjector the beam acquires an energy modulation because of the space charge effects and, if injected in a RF-compressor or in a magnetic chicane with negative R_{56} , the energy modulation can be transformed back into a density modulation [11]. Experimental results with two bunches after a RF compressor at SPARC are reported in refs. [10, 12]; the total bunch charge was ranging from 70 to 180 pC and the energy was varying from 164 to 110 MeV, depending on the injection phase in the bunch compressor.

Reference [13] investigates the machine settings for obtaining two micro-bunches tailored to the generation of a train of single spikes in an SASE-FEL experiment, useful

for pump and probe experiments. The use of a train of THz-repetition-rate ultrashort electron bunches to enhance THz radiation from Coherent Transition Radiation of the bunch train hitting a target, was first proposed in 2008 [14]; the first experimental results with a train of two bunches followed in 2010 [15] with two bunches separated of 0.7 ps with a total charge of 180 pC at 100 MeV.

A birefringent crystal to shape the laser pulse is adopted also by L. Yan *et al.* at Tsinghua university [16]; they are using four pieces of α -BBO crystals to separate an input UV pulse with appropriate duration into 16 sub-pulses to form a ps-spaced pulse train suitable for coherent THz production. Preliminary experimental results have been reported in ref. [17] on the production of ps-spaced bunch trains with up to four bunches at 2.8 MeV beam energy and with a total beam charge of 40–50 pC.

A completely different approach to produce THz repetition rate bunch trains is placing a mask in a high dispersion, low beta function region of a beam line dogleg in order to produce a temporal bunch train out of a long bunch with a correlated energy spread. The bunch train structure is very stable in time and energy because the mask is a fixed object in a dispersive section of a beam line; tailoring the bunch train shape is relatively easy as needed, for example, in Plasma Wake Field Acceleration (PWFA) schemes. Moreover the outcoming bunches are the ones which emittance is preserved and this scheme can be adopted in any application where high brightness beams are necessary. The drawback is that approximately 50% of the initial charge is lost in such a process and a charge not greater of 20 pC in each sub-bunch has been experimentally achieved at 58 MeV (see [18] and related references).

A THz repetition rate bunch train can also be generated with a transversely segmented beam (with a multislit mask) via a transverse-to-longitudinal phase space exchange technique, obtained placing a deflecting cavity between two dispersive sections. Such a scheme has been used to generate 14 MeV, five bunches train with total charge of 15 pC and applied to enhance narrow-band THz radiation emission from a transition radiation screen [19].

4. – General issues on comb beam manipulation

In order to focus on the main physical aspects of the comb bunch dynamics, fig. 1 shows the compression curve for a two bunches train from a TSTEP simulation [20] with parameters relevant for the SPARC linac. A 165 pC, a two sub-bunches (beam rms size of 145 fs) train is extracted from the cathode with a bunch distance of 4.27 ps and equally distributed charge; the RF gun boosts its energy up to 4.7 MeV and then the train enters the first TW section 1.5 meter after the cathode at different injection phase. The compression phase of fig. 1 refers to the difference from this injection phase and the “on crest” (maximum energy at the linac end) phase. The final energy of the beam depends on the compression phase and varies from 177 MeV (on crest situation) to roughly 100 MeV in over-compression (*i.e.* for compression phases more negative than the maximum compression one).

Figure 1 describes the longitudinal behavior of the whole bunch and of each sub-bunch (blue data refers to the bunch first hitting the cathode, red data to the other). The black (blue, red) line is the ratio between the bunch length on crest and the total (first, second) bunch length at different phases. One can see that the total bunch length decreases up to a minimum value (-98 deg) and the two bunches are in the same position as at the gun cathode. Increasing the compression phase, the sub-bunches invert their position and they start to become distinguishable and to increase their separation. The dynamics

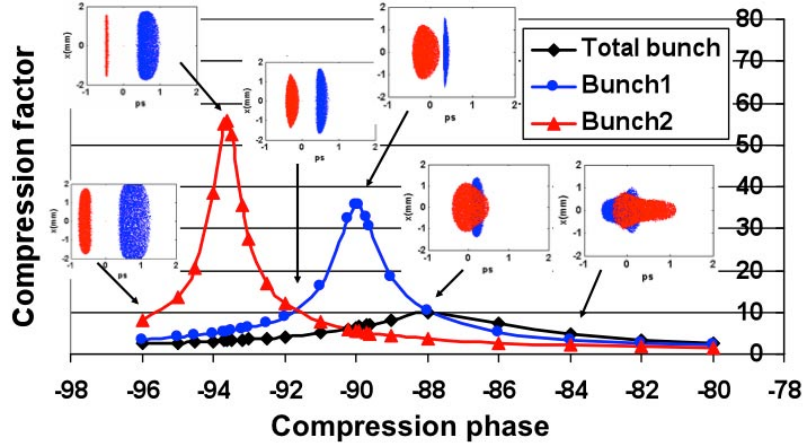


Fig. 1. – Compression curve for two-bunches pulse train at SPARC (TSTEP simulation, total charge 165 pC).

of each sub-bunch is anyway different; the first bunch reach its minimum length (max compression, 200 fs) while the second is still in a moderate compression regime. If some application need the same current in the two bunches, the working point is close to the interception of the two curve (not exactly at the interception because the bunch shape is different in compression or over-compression [21]). In this simulation, the bunches are well separated at compression phases smaller than -90 deg and the sub-bunch distance (not shown) depends more or less linearly with the compression phase in this region. An interesting range for the applications, *i.e.* 0.6–1.1 ps bunch spacing is obtained between -91 and -94 deg in this simulation.

It is clear that one has to operate in (deep) over-compression regime, which implies a careful machine optimization to preserve significantly low emittances. On top of that, the experimental reconstruction of the sub-bunches dynamics is not trivial, since the resolution needed to measure correctly the sub-bunches length is very demanding in terms of bunch length measurement resolution.

As a general rule of thumb, the bunch separation is roughly twice the total bunch length in this region and such separation is completely frozen at the end of the first 3 m TW section (the SPARC RF compressor). For a given compression phase, the pulse separation increases for increasing the laser pulses distance and the whole bunch charge.

The phase distance of the maxima of the sub-bunches compression curves (that is of the sub-bunches minimum length) depends mainly on the pulse distance at the entrance of the RF compressor which, for a given RF gun injection phase, is determined by the space charge: the pulse distance at the RF compressor entrance increases with bunch charge and moving the gun injection phase towards the phase of maximum charge extraction. Simulations show that such a phase separation of the maxima can be inferred from the pulse distance of the on crest beam at the linac end. The sub-bunches minimum length (and thus their maximum compression) is in general different, being identical only in the ideal case of no space charge beams injected with the same energy in the compressor.

The SPARC linac is composed by three 3m TW sections after the gun (the first one being the compressor) and the beam injection phase can be varied autonomously for each

section; usually the second and the third section are phased to get the maximum energy at the linac exit. By changing the last section phase (*i.e.* the whole beam energy), only the energy (and not the time) separation is affected; in particular there is no effect on the sub-bunches current distribution.

The difference between the sub-bunches charges at the cathode does not affect the separation at the linac exit (for a given compression phase), while it affects the sub-bunches currents and bunch lengths.

Emittance compensation during the RF compression requires focusing additional to the RF acceleration one, which in the SPARC case is provided by two 3m (independently powered) solenoids embedding the first two TW sections. Typically only the first solenoid is used at operation values in the range of 270–330 G (for all the data/simulation presented here). Such magnetic field has a negligible effect on the separation, while it affects the emittance (at the linac exit), the sub-bunches bunch length and current (but not the sub-bunches current ratio) and the compression phases corresponding to the single bunch compression curves maxima, which are (more or less) rigidly shifted.

As usual in RF gun-based linac, the main knob to control the emittance is the solenoid embedding the gun. Such a solenoid affects the emittance of the whole bunch as well as the one of the sub-bunches, but also the sub-bunches length (*i.e.* their currents). Typically the minimum emittance of the whole bunch, the minimum emittance of the single sub-bunches and an equal current in the sub-bunches occur at different values of the gun solenoid field; typically for the SPARC case, these values differ no more than roughly 300 G. As a rule of thumb, the minimum emittance of the whole bunch, the equal current and the minimum spot size at the linac exit occur for close values of the gun solenoid field. On top of that, simulations suggest that the minimum emittance of the whole bunch occurs when one of the two sub-bunches (which are transversely concentric) was forming a ring around the other at the linac exit; operationally this condition can be often observed (especially for “well behaved” beams) letting the beam propagating for roughly 5 meters after the linac without additional (quadrupole) focusing and therefore finding a starting point for emittance optimization.

A possible procedure, while operating the machine for comb bunches, may be the setting the bunch separation by choosing the compression phase and then the emittance optimization (with the gun solenoid) for a given value of the TW section magnetic focusing field.

Applying the previous considerations, experiments were performed with two bunches (200–400 pC) and four-bunches (200 pC) train [22]; the train average energy at the linac exit was varying from 170 to 90 MeV, depending on the machine setting, mainly the compression phase to tune the sub-bunches distance and the last section phase to tune the sub-bunches energy separation. The use of the RF compressor in the over-compression regime requires good beam quality (*i.e.* transverse emittance) and overall machine stability. A poor beam emittance would spoil the brilliance and/or would imply a too large beam to be manipulated; the compression phase stability is important to keep the separation in the comb beam constant during operation. The first goal was achieved with the increase of beam energy at the gun exit (best value being 6.2 MeV), while the compression stability largely profited of a dedicated chilling of the RF compressor.

The goal of most of the experiments was enhancing THz radiation by use of ps-spaced, hundreds of fs long sub-bunches; therefore most of our effort was oriented to obtain a stable longitudinal configuration with tunable bunch spacing. The transverse emittance optimization was addressed only to obtain a loss free transport in the dogleg line where the THz station was located. It is clear that, in order to use such beams in PWFA

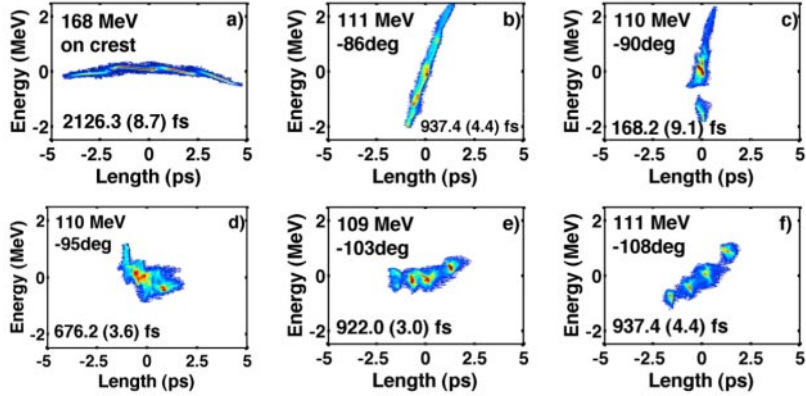


Fig. 2. – Four-comb pulse longitudinal phase space rotation; the label reports the average energy, the compression phase and the rms bunch length (200 pC).

oriented experiments, the transverse emittance is fundamental to allow proper focusing of the beam into the plasma.

5. – Four-bunches train

The LPS evolution of a four-bunch train in the RF compressor is shown in fig. 2: increasing the compression phase, the beam LPS rotates counter clockwise from the maximum linac exit energy (fig. 2.a), to the compression regime (fig. 2.b), then to maximum compression (fig. 2.c) thus entering the over-compression (fig. 2.d-f), very similarly to the two bunch case discussed in ref. [22].

The relevant regime for the application, *i.e.* where the sub-bunches are well separated and their distance can be tuned with the RF compressor injection phase, is after the phase when the minimum energy spread is reached (fig. 2.e) namely the “deep” over-compression (*e.g.* fig. 2.f).

We have carefully investigated this regime, both numerically and experimentally. As an example, fig. 3 shows another case of deep over-compression compared to TSTEP simulation, showing excellent agreement. The simulated LPSs are always thinner than the measured ones possibly due to RF deflector measurement issues (resolution and/or non-zero transverse emittance). One can see that the first two sub-bunches (on the left side of the picture) have a negative energy chirp while the other two have it much closer to zero. The first two sub-bunches of fig. 3 correspond to the ones entering later in the RF compressor (red particles in fig. 1). The energy chirp of the whole bunch and the sub-bunches energy separation can be tuned adjusting the beam entrance phase in the third accelerating section (while the sub-bunches current and spacing remain unchanged); the sub-bunches energy chirp is affected as well, but in a much smaller way.

As for the two bunches case, the longitudinal behavior of the whole bunches, as well as, of each sub-bunch has been analyzed deeply while only the whole bunch transverse emittance has been exhaustively studied. As predicted from simulation, the transverse emittance is less sensitive to the gun focusing field in the four sub-bunches case than with two sub-bunches; again the solenoid embedding the RF compressor was of primary importance. As a matter of fact, in deep over compression regime the horizontal

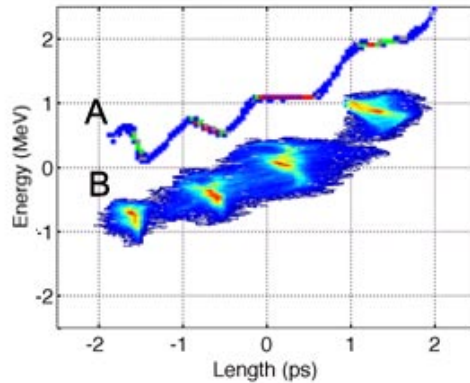


Fig. 3. – Comparison of measured longitudinal phase space (B) to simulated one (A). For reader convenience, the simulated LPS is artificially shifted up of 1 MeV to be distinguished from the measurements (200 pC).

emittance optimization (and measurement as well) was far more difficult than the vertical one. Table I reports typical values of $\sqrt{\varepsilon_x \varepsilon_y}$ (first three lines) and ε_y (last three lines) concerning the measurements shown in fig. 2-3.

6. – Application of comb beams

A number of application can profit of such comb beams: all of them require pulse separations < 1 ps and average currents in the range of hundreds amperes/bunch even if with some peculiarity different for each application.

For instance, one way to increase the accelerating field driven by an electron bunch in a PWFA (or in any collinear accelerator) is to modulate the current of the drive bunch and to resonantly drive the wakefield in a high-density plasma. In this case, the plasma wavelength must be equal to the bunch spacing. While this resonant excitation maximizes the accelerating wakefield amplitude, the transformer ratio, and therefore the energy transfer efficiency (from the drive train to the wakefield or to a trailing witness bunch), can be optimized by using a ramped bunch train method [23]. In that method, the charge is increased along the bunch train to keep the decelerating field the same for all drive bunches. Resonant excitation of plasma waves, thus, require well defined spacing, ramped bunch train for exciting ultrahigh gradients in PWFA.

TABLE I. – 90% transverse emittance (mm-mrad), 200 pC.

| | | |
|-----------------------|---------------|--------------|
| On crest | 1.114 (0.026) | see fig. 2.a |
| Compression | 1.802 (0.047) | see fig. 2.b |
| Max compression | 4.01 (0.11) | see fig. 2.c |
| Over compression | 3.78 (0.17) | see fig. 2.e |
| Deep over compression | 4.49 (0.16) | see fig. 2.f |
| Deep over compression | 4.09 (0.12) | see fig. 3 |

THz radiation production needs a well defined pulse spacing, reduced energy separation, equal pulses current. Coherent THz radiation is currently produced and optimized at SPARC-LAB through trains of ultra-short relativistic electron bunches as both transition and diffraction radiation. Different THz emission regimes, both broad band and narrow band, have been achieved by properly control electron beam shaping, length and charge of the comb beam [24-26].

Ultrafast pump-probe experiments at the femtosecond time scale can be done by exploiting the FEL radiation obtained by sending the comb beam in an undulator and thus producing a corresponding train of radiation pulses of variable delays and wavelengths; therefore an energy increasing or decreasing along the bunch train can be useful. First experimental results with a two pulses comb beam are reported in ref. [27]. In these experiments different spectrums as been acquired, showing as both the bunches were lasing. The characteristic of these spectrum to show fringes which are produced by two sources close in space and frequency. The interference fringes visibility change in a relevant way from shot to shot, and it is correlated to the bunches distance jitters into the train as to the energy produced.

7. – Conclusions

The comb scheme (comb laser pulse and RF compression) proposed in 2007 [11] is an active method to generate THz repetition rate bunch trains without the introduction of beam losses. We have demonstrated experimentally the control of pulse spacing, length, current and energy separation by properly setting the accelerator; currently, two pulses comb beams are used in THz radiation experiment as well as in FEL radiation generation. In this paper we have reported details on the manipulation of four sub-bunches train with a charge of 200 pC.

* * *

The author would like to thank all the people who contributed to this work, in particular the whole SPARC team. This work has been partially supported by the EU Commission in the Seventh Framework Program, Grant Agreement 312453 - EuCARD-2, Contract n. 283745-CRISP and by the Italian Ministry of Research in the framework of FIRB-Fondo per gli Investimenti della Ricerca di Base, Project no. RBFR12NK5K.

REFERENCES

- [1] ALESINI D. *et al.*, *Nucl. Instrum. Methods Phys Res. A*, **507** (2003) 345.
- [2] FERRARIO M. *et al.*, *Nucl. Instrum. Methods Phys. Res. B*, **309** (2013) 183.
- [3] FERRARIO M. *et al.*, *Phys. Rev. Lett.*, **99** (2007) 234801.
- [4] SERAFINI L. and FERRARIO M., *AIP Conf. Proc.*, **581** (2001) 87.
- [5] FILIPPETTO D. *et al.*, *Proceedings of FEL 2009*, **WOB01** (2009) 473.
- [6] CIANCHI A. *et al.*, *Phys. Rev. ST Accel. Beams*, **11** (2008) 032801.
- [7] MOSTACCI A. *et al.*, *Rev. Sci. Instrum.*, **79** (2008) 013303.
- [8] FERRARIO M. *et al.*, *Phys. Rev. Lett.*, **104** (2010) 054801.
- [9] GIANNESI L. *et al.*, *Phys. Rev. Lett.*, **106** (2011) 144801.
- [10] FERRARIO M. *et al.*, *Nucl. Instrum. Methods Phys. Res. A*, **637** (2010) S43.
- [11] BOSCOLO M. *et al.*, *Nucl. Instrum. Methods Phys. Res. A*, **577** (2007) 409.
- [12] FERRARIO M. *et al.*, *Proc. of IPAC10*, **TUPE082** (2010) 2311.
- [13] BOSCOLO M. *et al.*, *Nucl. Instrum. Methods Phys. Res. A*, **593** (2008) 116.
- [14] BOSCOLO M. *et al.*, *Proc. of EPAC08*, **WEPC069** (2008) 2154.

- [15] CHIADRONI E. *et al.*, *Proc. of IPAC10*, **TUOARA03** (2010) 1296.
- [16] YAN L. *et al.*, *Nucl. Instrum. Methods Phys. Res. A*, **637** (2010) S127.
- [17] YAN L. *et al.*, *Proc. of IPAC10*, **WEPD051** (2010) 3210.
- [18] MUGGLI P. *et al.*, *Phys. Rev. ST Accel. Beams*, **13** (2010) 052803.
- [19] PIOT P. *et al.*, *App. Phys. Lett.*, **98** (2011) 261501.
- [20] YOUNG L. *et al.*, private communication (2014).
- [21] FILIPPETTO D. *et al.*, *Phys. Rev. ST Accel. Beams*, **14** (2011) 092804.
- [22] MOSTACCI A. *et al.*, *Proc. of IPAC11*, **THYB01** (2011) 2877.
- [23] FERRARIO M., *Nucl. Instrum. Methods Phys. Res. B*, **309** (2013) 183.
- [24] CHIADRONI E. *et al.*, *Appl. Phys. Lett.*, **102** (2013) 094101.
- [25] CHIADRONI E. *et al.*, *Rev. Sci. Instrum.*, **84** (2013) 022703.
- [26] CHIADRONI E.,, this issue.
- [27] PETRILLO V. *et al.*, *Phys. Rev. Lett.*, **111** (2013) 114802.